Fourier Based MLFMM for the Helmholtz Equation

Cris Cecka Eric Darve

Department of Mechanical Engineering
Institute for Computational and Mathematical Engineering
Stanford University

May 20th, 2010
IV European Conference on Computational Mechanics

Solving Helmholtz

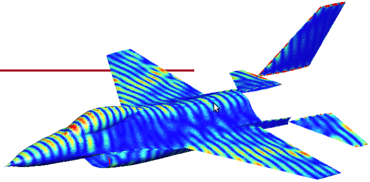

The Helmholtz equation over $\Omega \subset \mathbb{R}^3$,

$$(\nabla^2 + \kappa^2) u(\mathbf{x}) = \rho(\mathbf{x})$$

has solution

$$u(\mathbf{x}) = \int_\Omega \frac{e^{\imath\kappa|\mathbf{x}-\mathbf{y}|}}{4\pi\,|\mathbf{x}-\mathbf{y}|}\rho(\mathbf{y})\; d\mathbf{y}$$

Taking a set of point sources $\{\mathbf{y}_j\}_{j=1}^N$ and field points $\{\mathbf{x}_i\}_{i=1}^N$,

$$u(\mathbf{x}_i) = \sum_{\mathbf{y}_j \neq \mathbf{x}_i} \frac{e^{\imath\kappa|\mathbf{x}_i-\mathbf{y}_j|}}{4\pi\,|\mathbf{x}_i-\mathbf{y}_j|}\rho_j$$

requiring $\mathcal{O}(N^2)$ operations. MLFMM reduces this to $\mathcal{O}(N \log N)$.

Low Rank Approximation

The Helmholtz MLFMM is based on the plane wave expansion

$$\frac{e^{\imath\kappa|\mathbf{r}_0+\mathbf{r}|}}{|\mathbf{r}_0+\mathbf{r}|} = \lim_{\ell\to\infty} \int_{S^2} e^{\imath\kappa\langle\hat{\mathbf{s}},\mathbf{r}\rangle}\, T_{\ell,\mathbf{r}_0}(\hat{\mathbf{s}})\, \mathrm{d}S(\hat{\mathbf{s}})$$

• x_i

y_j •

Low Rank Approximation

The Helmholtz MLFMM is based on the plane wave expansion

$$\frac{e^{\imath\kappa|\mathbf{r}_0+\mathbf{r}|}}{|\mathbf{r}_0+\mathbf{r}|} = \lim_{\ell\to\infty} \int_{S^2} e^{\imath\kappa\langle\hat{\mathbf{s}},\mathbf{r}\rangle} \, T_{\ell,\mathbf{r}_0}(\hat{\mathbf{s}}) \, \mathrm{d}S(\hat{\mathbf{s}})$$

• x_i

y_j •

Low Rank Approximation

The Helmholtz MLFMM is based on the plane wave expansion

$$\frac{e^{\imath\kappa|\mathbf{r}_0+\mathbf{r}|}}{|\mathbf{r}_0+\mathbf{r}|} = \lim_{\ell\to\infty}\int_{S^2} e^{\imath\kappa\langle\hat{\mathbf{s}},\mathbf{r}\rangle}\, T_{\ell,\mathbf{r}_0}(\hat{\mathbf{s}})\,\mathrm{d}S(\hat{\mathbf{s}})$$

We define fields over the 2-sphere at the nodes of a tree:

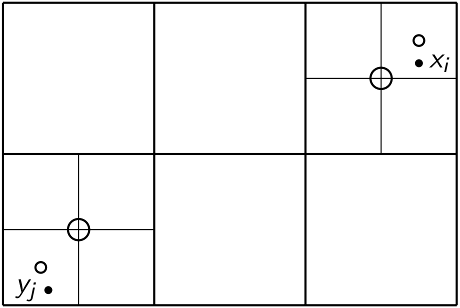

Low Rank Approximation

The Helmholtz MLFMM is based on the plane wave expansion

$$\frac{e^{\imath\kappa|\mathbf{r}_0+\mathbf{r}|}}{|\mathbf{r}_0+\mathbf{r}|} = \lim_{\ell\to\infty} \int_{S^2} e^{\imath\kappa\langle\hat{\mathbf{s}},\mathbf{r}\rangle}\, T_{\ell,\mathbf{r}_0}(\hat{\mathbf{s}})\, \mathrm{d}S(\hat{\mathbf{s}})$$

We define fields over the 2-sphere at the nodes of a tree:

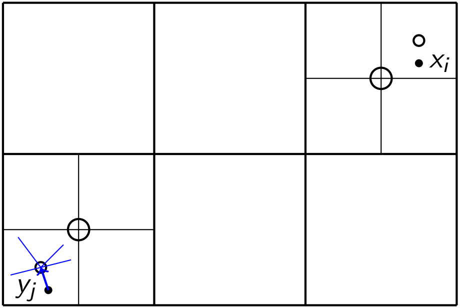

Low Rank Approximation

The Helmholtz MLFMM is based on the plane wave expansion

$$\frac{e^{\imath\kappa|\mathbf{r}_0+\mathbf{r}|}}{|\mathbf{r}_0+\mathbf{r}|} = \lim_{\ell\to\infty} \int_{S^2} e^{\imath\kappa\langle\hat{\mathbf{s}},\mathbf{r}\rangle}\, T_{\ell,\mathbf{r}_0}(\hat{\mathbf{s}})\, \mathrm{d}S(\hat{\mathbf{s}})$$

We define fields over the 2-sphere at the nodes of a tree:

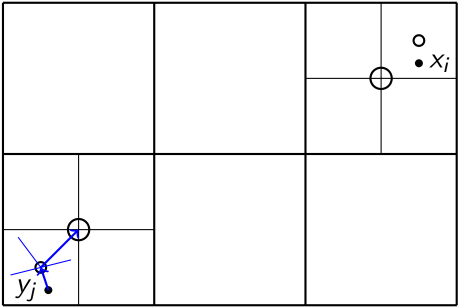

Low Rank Approximation

The Helmholtz MLFMM is based on the plane wave expansion

$$\frac{e^{\imath\kappa|\mathbf{r}_0+\mathbf{r}|}}{|\mathbf{r}_0+\mathbf{r}|} = \lim_{\ell\to\infty} \int_{S^2} e^{\imath\kappa\langle\hat{\mathbf{s}},\mathbf{r}\rangle}\, T_{\ell,\mathbf{r}_0}(\hat{\mathbf{s}})\, \mathrm{d}S(\hat{\mathbf{s}})$$

We define fields over the 2-sphere at the nodes of a tree:

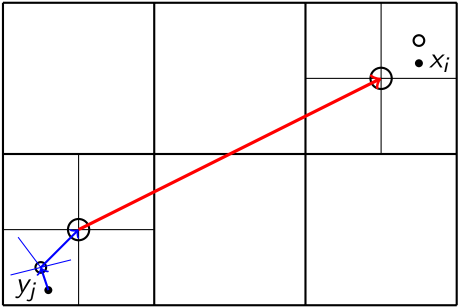

Low Rank Approximation

The Helmholtz MLFMM is based on the plane wave expansion

$$\frac{e^{\imath\kappa|\mathbf{r}_0+\mathbf{r}|}}{|\mathbf{r}_0+\mathbf{r}|} = \lim_{\ell\to\infty} \int_{S^2} e^{\imath\kappa\langle\hat{\mathbf{s}},\mathbf{r}\rangle}\, T_{\ell,\mathbf{r}_0}(\hat{\mathbf{s}})\, \mathrm{d}S(\hat{\mathbf{s}})$$

We define fields over the 2-sphere at the nodes of a tree:

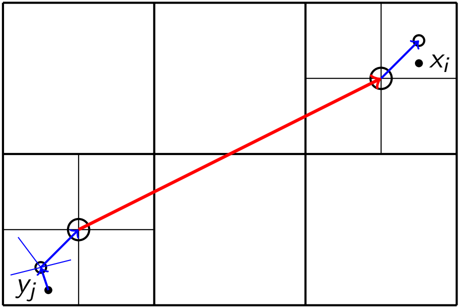

Low Rank Approximation

The Helmholtz MLFMM is based on the plane wave expansion

$$\frac{e^{\imath\kappa|\mathbf{r}_0+\mathbf{r}|}}{|\mathbf{r}_0+\mathbf{r}|} = \lim_{\ell\to\infty}\int_{S^2} e^{\imath\kappa\langle\hat{\mathbf{s}},\mathbf{r}\rangle}\, T_{\ell,\mathbf{r}_0}(\hat{\mathbf{s}})\,\mathrm{d}S(\hat{\mathbf{s}})$$

We define fields over the 2-sphere at the nodes of a tree:

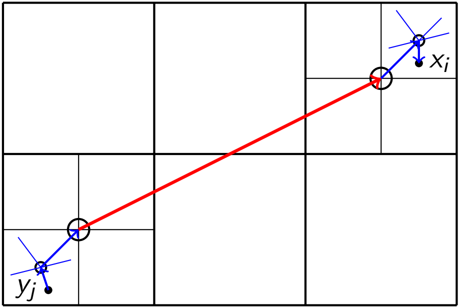

Typical Helmholtz MLFMM

- Field representation on S^2 - Spherical quadrature

Typical Helmholtz MLFMM

- Field representation on S^2 - Spherical quadrature
  - N Uniform in ϕ, $\frac{N}{2}$ Gauss-Legendre in $z(\theta)$.
  - Exactly integrates all Y_n^m, $|m| \leq n$, $n < N$.

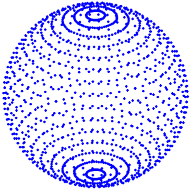

Typical Helmholtz MLFMM

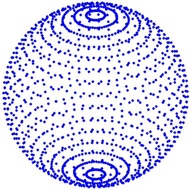

- Field representation on S^2 - Spherical quadrature
  - N Uniform in ϕ, $\frac{N}{2}$ Gauss-Legendre in $z(\theta)$.
  - Exactly integrates all Y_n^m, $|m| \le n$, $n < N$.
- Higher levels of the tree require larger quadrature.
  - $e^{\imath\kappa\langle \hat{\mathbf{s}},\mathbf{r}\rangle}$ has more frequencies when $|r|$ is large.

Typical Helmholtz MLFMM

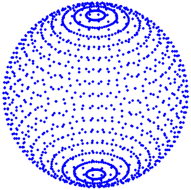

- Field representation on S^2 - Spherical quadrature
  - N Uniform in ϕ, $\frac{N}{2}$ Gauss-Legendre in $z(\theta)$.
  - Exactly integrates all Y_n^m, $|m| \leq n$, $n < N$.
- Higher levels of the tree require larger quadrature.
  - $e^{\imath\kappa\langle \hat{\mathbf{s}}, \mathbf{r}\rangle}$ has more frequencies when $|r|$ is large.
- Therefore, we must interpolate fields up the tree.
- Similarly, we must anterpolate fields down the tree.

Typical Helmholtz MLFMM

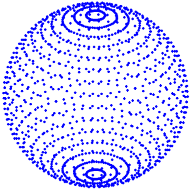

- Field representation on S^2 - Spherical quadrature
  - N Uniform in ϕ, $\frac{N}{2}$ Gauss-Legendre in $z(\theta)$.
  - Exactly integrates all Y_n^m, $|m| \leq n$, $n < N$.
- Higher levels of the tree require larger quadrature.
  - $e^{\imath\kappa\langle \hat{\mathbf{s}}, \mathbf{r}\rangle}$ has more frequencies when $|r|$ is large.
- Therefore, we must interpolate fields up the tree.
- Similarly, we must anterpolate fields down the tree.
- Typical Options:
  - Spherical Harmonic Transforms: Exact but Slow

Typical Helmholtz MLFMM

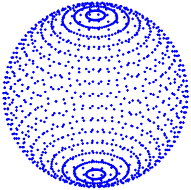

- Field representation on S^2 - Spherical quadrature
  - N Uniform in ϕ, $\frac{N}{2}$ Gauss-Legendre in $z(\theta)$.
  - Exactly integrates all Y_n^m, $|m| \leq n$, $n < N$.
- Higher levels of the tree require larger quadrature.
  - $e^{\imath\kappa\langle \hat{\mathbf{s}}, \mathbf{r} \rangle}$ has more frequencies when $|r|$ is large.
- Therefore, we must interpolate fields up the tree.
- Similarly, we must anterpolate fields down the tree.
- Typical Options:
  - Spherical Harmonic Transforms: Exact but Slow
  - Sparsified/Fast SHT: Error and Difficult

Typical Helmholtz MLFMM

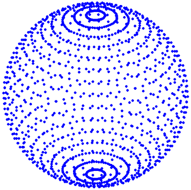

- Field representation on S^2 - Spherical quadrature
  - N Uniform in ϕ, $\frac{N}{2}$ Gauss-Legendre in $z(\theta)$.
  - Exactly integrates all Y_n^m, $|m| \leq n$, $n < N$.
- Higher levels of the tree require larger quadrature.
  - $e^{\imath\kappa\langle \hat{\mathbf{s}},\mathbf{r}\rangle}$ has more frequencies when $|r|$ is large.
- Therefore, we must interpolate fields up the tree.
- Similarly, we must anterpolate fields down the tree.
- Typical Options:
  - Spherical Harmonic Transforms: Exact but Slow
  - Sparsified/Fast SHT: Error and Difficult
  - Gauss/Lagrange/B-spline: Error/Speed Trade-off

Typical Helmholtz MLFMM

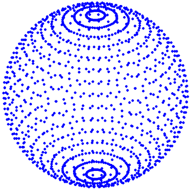

- Field representation on S^2 - Spherical quadrature
  - N Uniform in ϕ, $\frac{N}{2}$ Gauss-Legendre in $z(\theta)$.
  - Exactly integrates all Y_n^m, $|m| \leq n$, $n < N$.
- Higher levels of the tree require larger quadrature.
  - $e^{\imath\kappa\langle\hat{\mathbf{s}},\mathbf{r}\rangle}$ has more frequencies when $|r|$ is large.
- Therefore, we must interpolate fields up the tree.
- Similarly, we must anterpolate fields down the tree.
- Typical Options:
  - Spherical Harmonic Transforms: Exact but Slow
  - Sparsified/Fast SHT: Error and Difficult
  - Gauss/Lagrange/B-spline: Error/Speed Trade-off
- Moral: Want better interpolation/anterpolation.

Fourier Based Helmholtz MLFMM

Instead, use a 2D Fourier basis:

$$\int_{S^2} e^{\imath\kappa\langle \hat{\mathbf{s}},\mathbf{r}\rangle}\, T_{\ell,\mathbf{r}_0}(\hat{\mathbf{s}})\,\mathrm{d}S(\hat{\mathbf{s}}) = \int_0^{2\pi}\int_0^{2\pi} e^{\imath\kappa\langle \hat{\mathbf{s}},\mathbf{r}\rangle}\, T^{\mathfrak{s}}_{\ell,\mathbf{r}_0}(\hat{\mathbf{s}})\,\mathrm{d}\theta\,\mathrm{d}\phi$$

$$T^{\mathfrak{s}}_{\ell,\mathbf{r}_0}(\hat{\mathbf{s}}) = \frac{1}{2}\, T_{\ell,\mathbf{r}_0}(\hat{\mathbf{s}})\,|\sin(\phi)|$$

Fourier Based Helmholtz MLFMM

Instead, use a 2D Fourier basis:

$$\int_{S^2} e^{\imath\kappa\langle \hat{\mathbf{s}},\mathbf{r}\rangle}\, T_{\ell,\mathbf{r}_0}(\hat{\mathbf{s}})\,\mathrm{d}S(\hat{\mathbf{s}}) = \int_0^{2\pi}\int_0^{2\pi} e^{\imath\kappa\langle \hat{\mathbf{s}},\mathbf{r}\rangle}\, T^{\mathfrak{s}}_{\ell,\mathbf{r}_0}(\hat{\mathbf{s}})\,\mathrm{d}\theta\,\mathrm{d}\phi$$

$$T^{\mathfrak{s}}_{\ell,\mathbf{r}_0}(\hat{\mathbf{s}}) = \frac{1}{2}\, T_{\ell,\mathbf{r}_0}(\hat{\mathbf{s}})\,|\sin(\phi)|$$

- Fast, exact interpolation and anterpolation using FFTs.
- Uniform quadrature in $[0,2\pi]\times[0,\pi]$ (ϕ-symmetry)

Fourier Based Helmholtz MLFMM

Instead, use a 2D Fourier basis:

$$\int_{S^2} e^{\imath\kappa\langle \hat{\mathbf{s}},\mathbf{r}\rangle}\, T_{\ell,\mathbf{r}_0}(\hat{\mathbf{s}})\,\mathrm{d}S(\hat{\mathbf{s}}) = \int_0^{2\pi}\int_0^{2\pi} e^{\imath\kappa\langle \hat{\mathbf{s}},\mathbf{r}\rangle}\, T^{\mathfrak{s}}_{\ell,\mathbf{r}_0}(\hat{\mathbf{s}})\,\mathrm{d}\theta\,\mathrm{d}\phi$$

$$T^{\mathfrak{s}}_{\ell,\mathbf{r}_0}(\hat{\mathbf{s}}) = \frac{1}{2}\, T_{\ell,\mathbf{r}_0}(\hat{\mathbf{s}})\,|\sin(\phi)|$$

- Fast, exact interpolation and anterpolation using FFTs.
- Uniform quadrature in $[0, 2\pi] \times [0, \pi]$ (ϕ-symmetry)
- But requires a huge quadrature due to the high frequencies!

Fourier Based Helmholtz MLFMM

Instead, use a 2D Fourier basis:

$$\int_{S^2} e^{\imath\kappa\langle \hat{\mathbf{s}},\mathbf{r}\rangle}\, T_{\ell,\mathbf{r}_0}(\hat{\mathbf{s}})\,\mathrm{d}S(\hat{\mathbf{s}}) = \int_0^{2\pi}\int_0^{2\pi} e^{\imath\kappa\langle \hat{\mathbf{s}},\mathbf{r}\rangle}\, T^{\mathfrak{s}}_{\ell,\mathbf{r}_0}(\hat{\mathbf{s}})\,\mathrm{d}\theta\,\mathrm{d}\phi$$

$$T^{\mathfrak{s}}_{\ell,\mathbf{r}_0}(\hat{\mathbf{s}}) = \frac{1}{2}\, T_{\ell,\mathbf{r}_0}(\hat{\mathbf{s}})\,|\sin(\phi)|$$

- Fast, exact interpolation and anterpolation using FFTs.
- Uniform quadrature in $[0,2\pi]\times[0,\pi]$ (ϕ-symmetry)
- But requires a huge quadrature due to the high frequencies!
  - False.
  - Can be computed efficiently.
  - Can retain diagonality.

Fourier Based Helmholtz MLFMM

Consider a 1D analogue:

$$\mathcal{I} = \int_0^{2\pi} \Big[\sum_{n=-N}^{N} a_n e^{\imath n\phi} \Big] \Big[\sum_{m=-M}^{M} b_m e^{\imath m\phi} \Big] \, \mathrm{d}\phi \qquad M \gg N$$

Fourier Based Helmholtz MLFMM

Consider a 1D analogue:

$$\mathcal{I} = \int_0^{2\pi} \Big[\sum_{n=-N}^{N} a_n e^{\imath n\phi} \Big] \Big[\sum_{m=-M}^{M} b_m e^{\imath m\phi} \Big] \, \mathrm{d}\phi \qquad M \gg N$$

By Parseval's theorem, the frequencies $m > N$ do not contribute,

$$= \int_0^{2\pi} \Big[\sum_{n=-N}^{N} a_n e^{\imath n\phi} \Big] \Big[\sum_{m=-N}^{N} b_m e^{\imath m\phi} \Big] \, \mathrm{d}\phi$$

Can be computed exactly with $2N$ uniform points.

Fourier Based Helmholtz MLFMM

Consider a 1D analogue:

$$\mathcal{I} = \int_0^{2\pi} \Big[\sum_{n=-N}^{N} a_n e^{\imath n\phi} \Big] \Big[\sum_{m=-M}^{M} b_m e^{\imath m\phi} \Big] \, \mathrm{d}\phi \qquad M \gg N$$

By Parseval's theorem, the frequencies $m > N$ do not contribute,

$$= \int_0^{2\pi} \Big[\sum_{n=-N}^{N} a_n e^{\imath n\phi} \Big] \Big[\sum_{m=-N}^{N} b_m e^{\imath m\phi} \Big] \, \mathrm{d}\phi$$

Can be computed exactly with $2N$ uniform points.

- Similarly, $e^{\imath\kappa\langle \hat{\mathbf{s}},\mathbf{r}\rangle}$ has an effective bandwidth of $\mathcal{O}(\kappa\,|r|)$.

Fourier Based Helmholtz MLFMM

Consider a 1D analogue:

$$\mathcal{I} = \int_0^{2\pi} \left[\sum_{n=-N}^{N} a_n e^{\imath n\phi} \right] \left[\sum_{m=-M}^{M} b_m e^{\imath m\phi} \right] \mathrm{d}\phi \qquad M \gg N$$

By Parseval's theorem, the frequencies $m > N$ do not contribute,

$$= \int_0^{2\pi} \left[\sum_{n=-N}^{N} a_n e^{\imath n\phi} \right] \left[\sum_{m=-N}^{N} b_m e^{\imath m\phi} \right] \mathrm{d}\phi$$

Can be computed exactly with $2N$ uniform points.

- Similarly, $e^{\imath\kappa\langle \hat{\mathbf{s}}, \mathbf{r} \rangle}$ has an effective bandwidth of $\mathcal{O}(\kappa\,|r|)$.
- Remove frequencies of $T^{\mathfrak{s}}_{\ell,\mathbf{r}_0}(\hat{\mathbf{s}})$ which do not contribute.

Fourier Based Helmholtz MLFMM

Consider a 1D analogue:

$$\mathcal{I} = \int_0^{2\pi} \left[\sum_{n=-N}^{N} a_n e^{\imath n\phi} \right] \left[\sum_{m=-M}^{M} b_m e^{\imath m\phi} \right] \mathrm{d}\phi \qquad M \gg N$$

By Parseval's theorem, the frequencies $m > N$ do not contribute,

$$= \int_0^{2\pi} \left[\sum_{n=-N}^{N} a_n e^{\imath n\phi} \right] \left[\sum_{m=-N}^{N} b_m e^{\imath m\phi} \right] \mathrm{d}\phi$$

Can be computed exactly with $2N$ uniform points.

- Similarly, $e^{\imath\kappa\langle \hat{\mathbf{s}}, \mathbf{r}\rangle}$ has an effective bandwidth of $\mathcal{O}(\kappa\,|r|)$.
- Remove frequencies of $T^{\mathfrak{s}}_{\ell,\mathbf{r}_0}(\hat{\mathbf{s}})$ which do not contribute.
  - Make $T^{\mathfrak{s}}_{\ell,\mathbf{r}_0}(\hat{\mathbf{s}})$ band-limited with $\mathcal{O}(\kappa\,|r|)$ frequencies.
  - Easy since $T_{\ell,\mathbf{r}_0}$ has bandwidth ℓ and

$$\mathcal{F}(m; |\sin(\theta)|) = \frac{(-1)^m + 1}{\pi(1 - m^2)}$$

Improved Error Analysis

With exact integration and interpolation, only two sources of error:

$$\frac{e^{\imath\kappa|\mathbf{r}_0+\mathbf{r}|}}{|\mathbf{r}_0+\mathbf{r}|} \xrightarrow{1} \iint_0^{2\pi} e^{\imath\kappa\langle\hat{\mathbf{s}},\mathbf{r}\rangle}\, T^{\mathfrak{s}}_{\ell,\mathbf{r}_0}(\hat{\mathbf{s}})\,\mathrm{d}\theta\,\mathrm{d}\phi$$
$$\xrightarrow{2} \sum_k \omega_k e^{\imath\kappa\langle\hat{\mathbf{s}}_k,\mathbf{r}\rangle}\, T^{\mathfrak{s},L}_{\ell,\mathbf{r}_0}(\hat{\mathbf{s}}_k)$$

- Error 1 - Gegenbauer series truncation.
- Error 2 - Numerical quadrature approximation.

Improved Error Analysis

With exact integration and interpolation, only two sources of error:

$$\frac{e^{\imath\kappa|\mathbf{r}_0+\mathbf{r}|}}{|\mathbf{r}_0+\mathbf{r}|} \xrightarrow{1} \iint_0^{2\pi} e^{\imath\kappa\langle\hat{\mathbf{s}},\mathbf{r}\rangle}\, T_{\ell,\mathbf{r}_0}^{\mathfrak{s}}(\hat{\mathbf{s}})\,\mathrm{d}\theta\,\mathrm{d}\phi$$
$$\xrightarrow{2} \sum_k \omega_k e^{\imath\kappa\langle\hat{\mathbf{s}}_k,\mathbf{r}\rangle}\, T_{\ell,\mathbf{r}_0}^{\mathfrak{s},L}(\hat{\mathbf{s}}_k)$$

- Error 1 - Gegenbauer series truncation.
    - Well studied and easy to compute.
- Error 2 - Numerical quadrature approximation.

Improved Error Analysis

With exact integration and interpolation, only two sources of error:

$$\frac{e^{\imath\kappa|\mathbf{r}_0+\mathbf{r}|}}{|\mathbf{r}_0+\mathbf{r}|} \xrightarrow{1} \iint_0^{2\pi} e^{\imath\kappa\langle\hat{\mathbf{s}},\mathbf{r}\rangle} T_{\ell,\mathbf{r}_0}^{\mathfrak{s}}(\hat{\mathbf{s}})\,\mathrm{d}\theta\,\mathrm{d}\phi$$

$$\xrightarrow{2} \sum_k \omega_k e^{\imath\kappa\langle\hat{\mathbf{s}}_k,\mathbf{r}\rangle} T_{\ell,\mathbf{r}_0}^{\mathfrak{s},L}(\hat{\mathbf{s}}_k)$$

- Error 1 - Gegenbauer series truncation.
  - Well studied and easy to compute.
- Error 2 - Numerical quadrature approximation.
  - Account for error in $T_{\ell,\mathbf{r}_0}^{\mathfrak{s}} \longrightarrow T_{\ell,\mathbf{r}_0}^{\mathfrak{s},L}$.
  - Account for error in sampling $e^{\imath\kappa\langle\hat{\mathbf{s}}_k,\mathbf{r}\rangle}$ in finite quadrature.

Improved Error Analysis

With exact integration and interpolation, only two sources of error:

$$\frac{e^{\imath\kappa|\mathbf{r}_0+\mathbf{r}|}}{|\mathbf{r}_0+\mathbf{r}|} \xrightarrow{1} \iint_0^{2\pi} e^{\imath\kappa\langle\hat{\mathbf{s}},\mathbf{r}\rangle}\, T_{\ell,\mathbf{r}_0}^{\mathfrak{s}}(\hat{\mathbf{s}})\, \mathrm{d}\theta\, \mathrm{d}\phi$$

$$\xrightarrow{2} \sum_k \omega_k e^{\imath\kappa\langle\hat{\mathbf{s}}_k,\mathbf{r}\rangle}\, T_{\ell,\mathbf{r}_0}^{\mathfrak{s},L}(\hat{\mathbf{s}}_k)$$

- Error 1 - Gegenbauer series truncation.
  - Well studied and easy to compute.
- Error 2 - Numerical quadrature approximation.
  - Account for error in $T_{\ell,\mathbf{r}_0}^{\mathfrak{s}} \longrightarrow T_{\ell,\mathbf{r}_0}^{\mathfrak{s},L}$.
  - Account for error in sampling $e^{\imath\kappa\langle\hat{\mathbf{s}}_k,\mathbf{r}\rangle}$ in finite quadrature.
  - Want to find the smallest quadrature for a given accuracy.
  - Spectral analysis yields constructive algorithms for quadrature.

Quadrature Example

With $\kappa\,|\mathbf{r}| = 10$, a 1042 point quadrature is created:

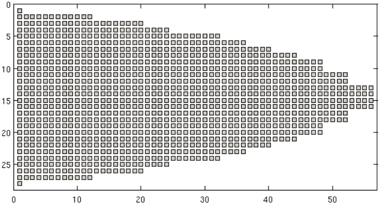

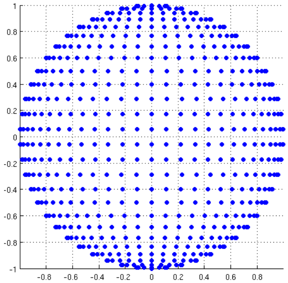

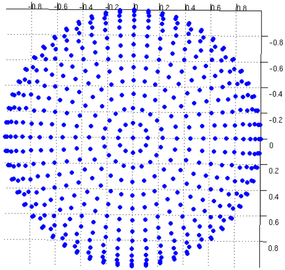

Interpolation/Anterpolation Between Quadratures

Interpolate/Anterpolate from quadrature Q to Q'. Let

$$\mathcal{N}_\phi = \max\left(\max_{1 \le j \le N_\theta} N_\phi(\theta_j), \ \max_{1 \le j \le N'_\theta} N'_\phi(\theta_j) \right)$$

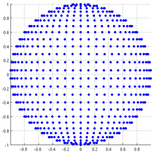

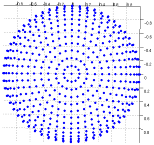

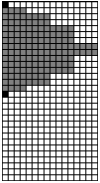

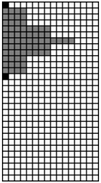

Interpolation/Anterpolation Between Quadratures

Interpolate/Anterpolate from quadrature Q to Q'. Let

$$\mathcal{N}_\phi = \max\left(\max_{1 \le j \le N_\theta} N_\phi(\theta_j),\ \max_{1 \le j \le N'_\theta} N'_\phi(\theta_j) \right)$$

1. Interpolate $N_\phi(\theta_j)$ to $\mathcal{N}_\phi$.

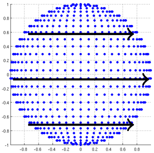

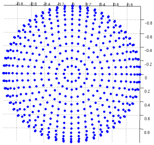

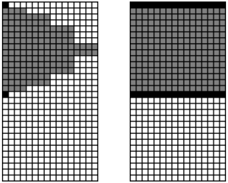

Interpolation/Anterpolation Between Quadratures

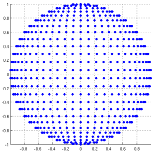

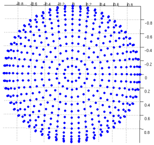

Interpolate/Anterpolate from quadrature Q to Q'. Let

$$\mathcal{N}_\phi = \max\left(\max_{1 \le j \le N_\theta} N_\phi(\theta_j), \ \max_{1 \le j \le N'_\theta} N'_\phi(\theta_j) \right)$$

1. Interpolate $N_\phi(\theta_j)$ to $\mathcal{N}_\phi$.
2. Wrap the data to construct the θ-periodic data.

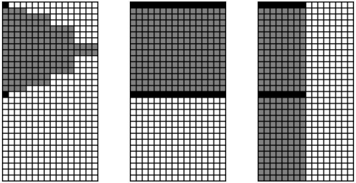

Interpolation/Anterpolation Between Quadratures

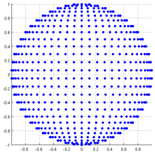

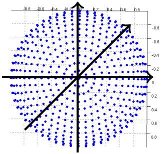

Interpolate/Anterpolate from quadrature Q to Q'. Let

$$\mathcal{N}_\phi = \max\left(\max_{1 \le j \le N_\theta} N_\phi(\theta_j), \; \max_{1 \le j \le N'_\theta} N'_\phi(\theta_j) \right)$$

1. Interpolate $N_\phi(\theta_j)$ to $\mathcal{N}_\phi$.
2. Wrap the data to construct the θ-periodic data.
3. Interpolate from length N_θ to N'_θ.

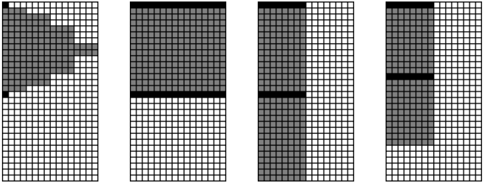

Interpolation/Anterpolation Between Quadratures

Interpolate/Anterpolate from quadrature Q to Q'. Let

$$\mathcal{N}_\phi = \max\left(\max_{1 \le j \le N_\theta} N_\phi(\theta_j), \max_{1 \le j \le N'_\theta} N'_\phi(\theta_j) \right)$$

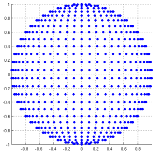

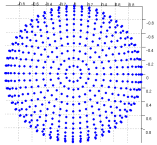

1. Interpolate $N_\phi(\theta_j)$ to $\mathcal{N}_\phi$.
2. Wrap the data to construct the θ-periodic data.
3. Interpolate from length N_θ to N'_θ.
4. Unwrap the data to construct the ϕ-periodic data.

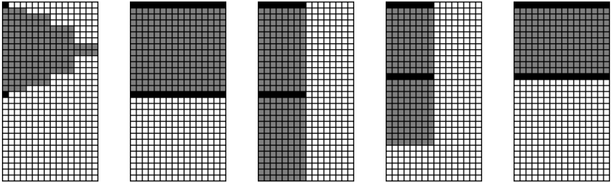

Interpolation/Anterpolation Between Quadratures

Interpolate/Anterpolate from quadrature Q to Q'. Let

$$\mathcal{N}_\phi = \max\left(\max_{1 \le j \le N_\theta} N_\phi(\theta_j), \ \max_{1 \le j \le N'_\theta} N'_\phi(\theta_j) \ \right)$$

1. Interpolate $N_\phi(\theta_j)$ to $\mathcal{N}_\phi$.
2. Wrap the data to construct the θ-periodic data.
3. Interpolate from length N_θ to N'_θ.
4. Unwrap the data to construct the ϕ-periodic data.
5. Anterpolate from length $\mathcal{N}_\phi$ to $N'_\phi(\theta_j)$.

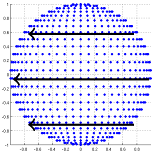

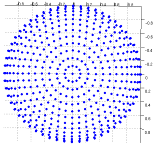

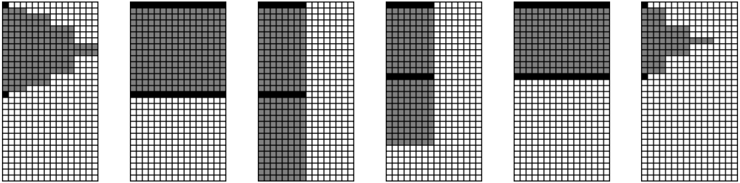

Error Results

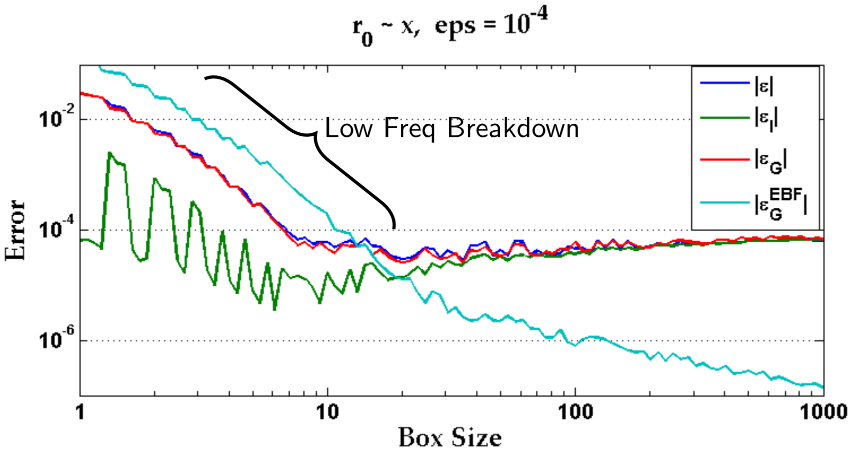

Error Results

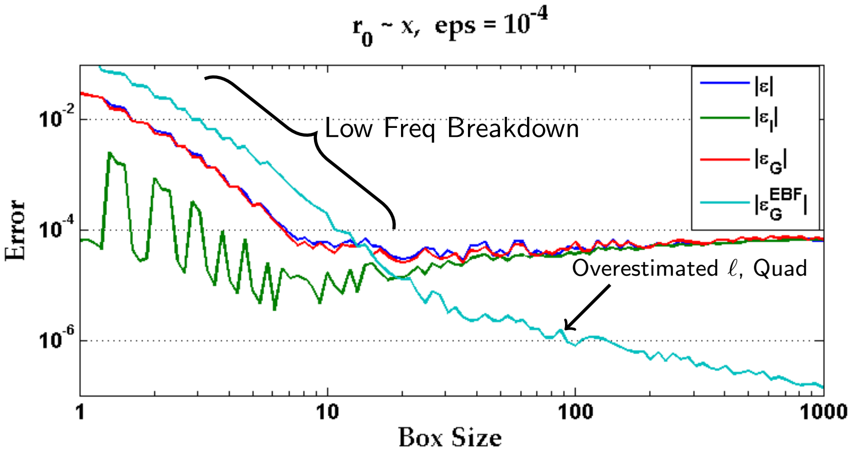

Asymptotic Running Time

With accuracy approximately 10^{-6},

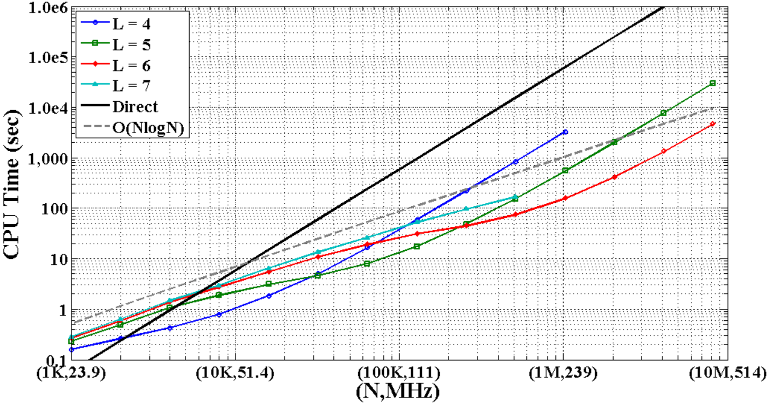

Moral of the Story

Reasons to use the Fourier Based FMM:

- Exact interpolation/anterpolation steps
- Fast with widely available, highly optimized FFT libraries
- Easier to implement - (Uniform quadrature, FFTs, etc)
- All error can be accounted for in the precomputation stage
  - Strict error bounds to be computed before the computation.
  - Error bounds are used to determine truncation and quadrature.